J. Biochem. **135**, 25–31 (2004)
DOI: 10.1093/jb/mvh003

Effects of Deletion and Shift of the A20–B19 Disulfide Bond on the Structure, Activity, and Refolding of Proinsulin

Zhao-Hui Wang, Ying Liu, Jian-Guo Ji* and Jian-Guo Tang

National Laboratory of Protein Engineering and Plant Genetic Engineering, College of Life Sciences, Peking University, Beijing, 100871, People's Republic of China

Received September 23, 2003; accepted October 27, 2003

To investigate the role of the A20–B19 disulfide bond in the structure, activity and folding of proinsulin, a human proinsulin (HPI) mutant [A20, B19Ala]-HPI was prepared. This mutant, together with another proinsulin mutant previously constructed with an A19Tyr deletion, which can also be taken as shifted mutant of the A20–B19 disulfide bond, were studied for their *in vitro* refolding, oxidation of free thiol groups, circular dichroism spectra, antibody and receptor binding activities and sensitivity to trypsin digestion in comparison with native proinsulin. The results indicate that deletion of the A20–B19 disulfide bond results in a large decrease in the α-helix content of the molecule and higher sensitivity to tryptic digestion. Both the deletion and shift mutations, especially the latter, cause a great decrease in the biological activity of proinsulin analogues. The folding yields of HPI analogues were much lower than that of HPI. And the shift mutant, [ΔA19Tyr]-HPI, was scarcely refolded correctly *in vitro* and its refolding yield was extremely low. These results suggest that the A20–B19 disulfide bond plays an important role in the structural stabilization and folding of the insulin precursor. By summarizing the refolding studies on proinsulin, a possible folding pathway is proposed.

Key words: biological activity, disulfide bond, proinsulin analogue, protein folding, secondary stucture.

Abbreviations: DTNB, 5,5′-dithio-bis-(2-nitrobenzonic acid); FPLC, fast protein liquid chromatography; HPI, human proinsulin; IGF-I, insulin-like growth factor I; LB, Luria Bertant medium; MALDI-TOF MS, matrix-assisted laser desorption and ionization time-of-flight mass spectrometry; RPC, reverse phase chromatography; TFA, trifluoroacetic acid.

The three motif-specific disulfide bonds of insulin and insulin-related proteins have drawn much attention to their impact on the structure, activity and precursor folding pathways of these proteins. The roles of the disulfide bonds in the folding of IGF-I have been well-established (*1–4*). Among the three disulfide bonds in IGF-I, the 18–61 disulfide bond (corresponding to the A20–B19 interchain disulfide bond in insulin) was proposed to form first in the folding pathway (*1*). An IGF-I mutant with only the 18–61 disulfide bond is still in a compact, partially folded state, with low but significant biological activity (*2*). In order to understand the roles of disulfide bonds in the folding and biological activity of insulin/proinsulin, many deletion as well as shift mutations have been introduced to the A6–A11 and A7–B7 disulfide bonds (*5–12*). However, mutant recombinant insulin precursors without the A20–B19 disulfide bond fail to be secreted from transformed yeast cells (*9*). No mutant protein is available for study, although a very important role of the A20–B19 disulfide bond in efficient folding/secretion *in vivo* was inferred. Intermediates containing the native A20–B19 disulfide bond were found in the *in vitro* refolding of recombinant porcine insulin precursor (PIP), and also recently in the *in vitro* refolding of human proinsulin (*13*, *14*). Recently, a PIP mutant with only the A20–B19 disulfide bond was constructed, which can be secreted from yeast cells with decreased secretion yield and adopts a partially folded conformation (*15*). All the previous studies suggest that the A20–B19 inter-chain disulfide bond may play an important role in the structure stabilization and folding of insulin precursor. In order to study the role of the A20–B19 disulfide bond more directly, we constructed an A20–B19 deleted mutant [A20, B19Ala]-HPI by replacing the cysteine residues at both the A20 and B19 positions in human proinsulin (HPI) with alanine. The mutant protein was successfully prepared by expression as inclusion body in *Escherichia coli* and refolding *in vitro*. The physico-chemical properties and biological activities as well as the *in vitro* refolding behaviors of the [A20, B19Ala]-HPI mutant protein along with those of another previously constructed HPI mutant, [ΔA19Tyr]-HPI (*16*), which can also be regarded as an HPI mutant with a shift mutation at the A20-B19 disulfide bond, were studied and compared with those of HPI. The disulfide bond patterns of HPIs used in this paper are shown in Fig. 1A. The three-dimensional structure of insulin with three disulfide bonds is shown in Fig. 1B.

MATERIALS AND METHODS

Materials—E. coli DH5α was used as host for the expression of recombinant genes. Plasmid pBV220, with λ-phage CI heat-shock promoter P_RP_L, was used as clon-

*To whom correspondence should be addressed. Fax: +86-10-6275-1526, E-mail: jijg@pku.edu.cn

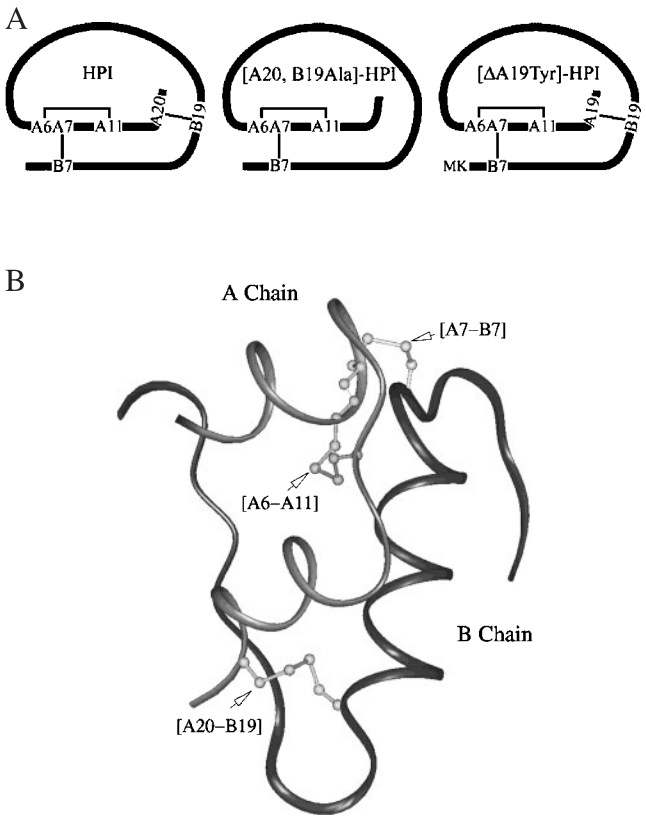

Fig. 1. **Demonstration of some insulin disulfide bond related structures.** (A) illustration of disulfide bonds in HPI and its two analogues. The known disulfide linkages in HPI and the probable disulfide linkages in the analogues are shown. (B) three-dimensional structure of insulin with three disulfide bonds. The structure was derived from 2HIU in the protein databank (Brookheaven, CA) by the program Insight II.

ing vector. pJG103 containing the *HPI* gene, and a plasmid containing the [ΔA19Tyr]-*HPI* gene were previously constructed in our laboratory (*16*, *17*). PCR primers for the construction of HPI mutant genes were synthesized by Sagon, Shanghai. Taq DNA polymerase, T_4 DNA ligase and restrictive enzymes were Promega products. DTT was purchased from Sagon, Shanghai. Endoproteinase Glu-C (V8) of sequencing grade and trypsin with an activity of 10,400 units/mg were Sigma products. Chromatography columns and media were products of Amersham Pharmacia, Sweden. DTNB and other chemicals of analytical or chromatographic grade were local products. The [^{125}I]-insulin radioimmunoassay kit was kindly provided by Navy Radioimmunoassay Technique Center (Beijing, China).

Mutant Gene Construction and Protein Preparation—The mutant gene of [A20, B19Ala]-HPI was obtained by PCR with plasmid pJG103 containing the *HPI* gene as template. The mutant primers (5′-gaggaattccggatg tttgtcaatcagcacctttgtggttctcacctggtggaggccttgtacctggtg**gc**tgggggaacgt-3′ and 5′-aggggatcctcagtt**agc**gtagttctcc-3′) introduced Cys→Ala mutations at both the A20 and B19 positions of *HPI*. The mutant gene was then inserted into pBV220 and the constructed expression plasmid was used to transform *E. coli* strain DH5α. The target mutations were confirmed by DNA sequencing. The constructed [A20, B19Ala]-*HPI* as well as *HPI* and [ΔA19Tyr]-*HPI* were expressed, and protein monomers were obtained following the procedures described in (*17*), and purified on an RPC Resource™ (3 ml) column. The RPC column was equilibrated with distilled water containing 0.1%TFA, and eluted with a linear gradient of 0–100% acetonitrile containing 0.1% TFA at 2 ml/min for 10 column volumes. The purified proteins with purities greater than 95% were lyophilized and stored at –20°C for later testing.

Identification of Disulfide Match by V8 Mapping—Ten micrograms of HPI or [ΔA19Tyr]-HPI was digested with 0.5 μg of endoproteinase V8. Enzymatic digestion was performed in 0.1 M Tris-HCl (pH 7.8) at 37°C for 18 h. A 0.5-μl aliquot of the digest solution was mixed with 0.5 μl of matrix (saturated α-cyanocinnamic acid in 30% aqueous acetonitrile) and subjected to MALDI-TOF MS using a Bruker Biflex™ III instrument (Bremen, German) in linear mode at 19 kV.

In Vitro Refolding Assay of Fully Reduced Proteins—One milligram of HPI or its analogues were dissolved in 1 ml of 0.05 M Tris-HCl (pH 8.0), containing 8 M urea, 1 mM EDTA and 20-fold (in terms of thiol groups) excess DTT. After incubation at 37°C for 2 h, the reaction mixture was dialyzed against 2000 volumes of refolding buffer (0.05 M glycine-NaOH, pH 10.8) at 4°C for 24 h to remove reducing reagent and denaturant. Ten microliters of each refolding product was then analyzed by both 15% native PAGE and 15% non-reductive SDS-PAGE. After staining the gel with Coomassie Brilliant Blue, the proinsulin bands were quantified by densitometry using Glyko Bandscan software (Glyko, USA).

Measurement of Thiol Group Oxidation—Two milligrams of HPI or its analogues were dissolved in 1 ml of 0.05 mol/liter Tris-HCl (pH 8.0), containing 8 mM urea, 1 mM EDTA, and 20-fold (in terms of thiol group) excess DTT. After incubation at 37°C for 2 h, the pH of the reaction mixture was adjusted to 2–3 and the reaction mixture was loaded onto a desalting FPLC HiTrap™ column (5 ml). The column was eluted with 0.1% TFA to remove excess DTT. The collected protein peak was mixed with 1/10 volume 0.5 M glycine-NaOH (pH 10.8) and incubated at 4°C for refolding. The numbers of thiol groups at various time periods during refolding were determined with DTNB according to Ellman's method (*18*).

CD Studies—HPI or its analogues were dissolved in double-distilled water (pH 7.0). Protein concentration was determined by UV absorbency and adjusted to 0.2 mg/ml. CD measurement was performed on a Jasco-715 circular dichroism spectropolarimeter with a cell pathlength of 2 mm. The spectrum was recorded at 25°C and was the average of four scans from 200 to 250 nm. The relative secondary structure contents were calculated according to the method of Chen & Yang (*19*).

Receptor and Antibody Binding Activities Assay—The receptor binding activity assay of mutant HPI was performed as described previously (*20*). The immune assay with insulin polyclonal antibodies was performed according to the manual for the [^{125}I]-insulin radioimmunoassay kit.

Sensitivity to Tryptic Digestion Assay—Two milligrams of HPI or its analogues were dissolved in 1 ml of 0.05 M Tris-HCl, pH 7.2. Trypsin was dissolved at different concentrations in 1 mM HCl, and 2 μl of trypsin was then

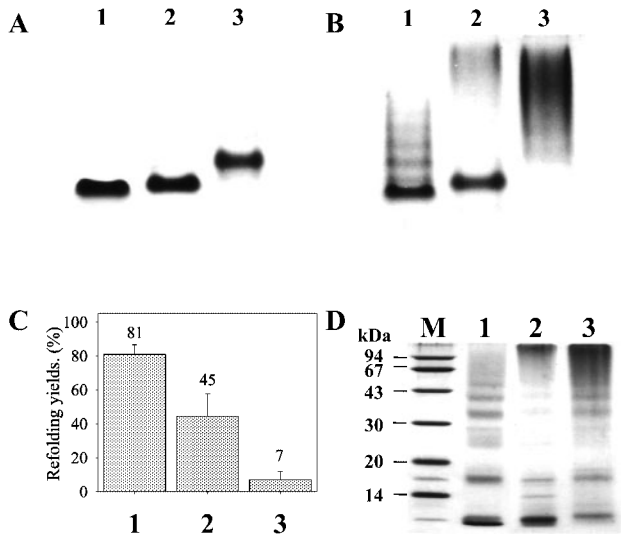

Fig. 2. **Refolding analysis of HPI and its analogues.** (A) 15% native PAGE analysis of purified HPI and its analogues. (B) 15% native PAGE analysis of HPI and its analogues after *in vitro* refolding. (C) refolding yields of HPI and its analogues under the given conditions. The values represent mean ± SD of three independent experiments as shown in (B). (D) 15% non-reductive SDS-PAGE analysis of HPI and its analogues after *in vitro* refolding. In each panel, 1, 2, 3 represent HPI, [A20, B19Ala]-HPI, and [ΔA19Tyr]-HPI, respectively.

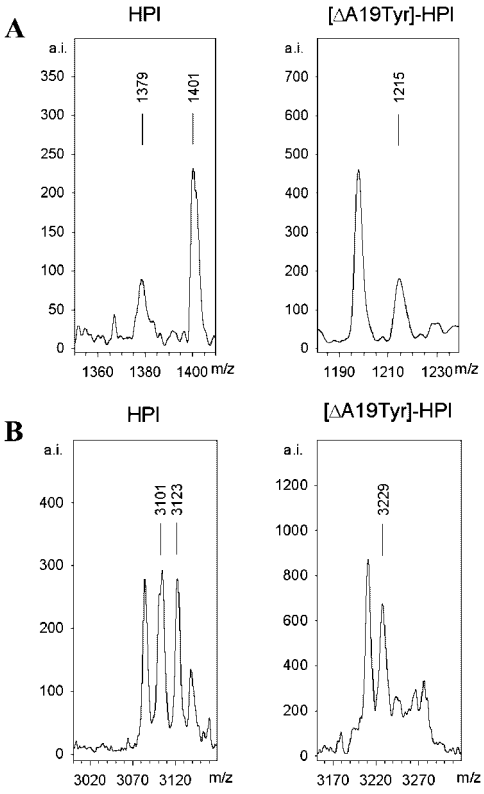

Fig. 3. **MALDI-TOF MS analysis of the products of V8 digested HPI and [ΔA19Tyr]-HPI.** (A) Peaks corresponding to A (18–21)/B (14–21) for HPI and peaks corresponding to A (18–20)/B (14–21) for [ΔA19Tyr]-HPI. Measured MH^+ are indicated. The theoretical MH^+ for HPI and [ΔA19Tyr]-HPI are 1,378.5 and 1,215.4, respectively. The theoretical MNa^+ for HPI is 1,400.5. (B) Peaks corresponding to A (5–17)/Met + B (1–13) for HPI and peaks corresponding to A (5–17)/Met + Lys + B (1–13) for [ΔA19Tyr]-HPI. Measured MH^+ are indicated. The theoretical MH^+ for HPI and [ΔA19Tyr]-HPI are 3,101.5 and 3,229.8, respectively. The theoretical MNa^+ for HPI is 3,123.5.

added to 20 μl of HPI or its analogue solution at defined enzyme/substrate (w/w) ratios. After incubation at 37°C for 0.5 h, the reaction was stopped by adding an equal volume of 2× native PAGE loading buffer. A 10-μl aliquot of reaction mixture was subjected immediately to 15% native PAGE. The corresponding des-B30Thr-insulin bands were quantified by Glyko Bandscan software.

RESULTS

Identification of Disulfide Linkage of [ΔA19Tyr]-HPI—HPI and HPI analogues with deletion and shift mutations in the A20–B19 disulfide bond purified by reverse phase FPLC appeared as single major band on native PAGE gel (Fig. 2A). The mobility rate of [A20, B19Ala]-HPI was a little slower than that of HPI, while [ΔA19Tyr]-HPI showed a much slower mobility rate, which may be a result of the positive charge provided by the additional lysine in the N-terminus (*16*). The protein also showed single peaks on reverse phase FPLC analysis (data not shown). HPI and [ΔA19Tyr]-HPI were digested with V8 and analyzed by MALDI-TOF MS. For HPI, two proteolytic segments with [A6-A11, A7-B7] and [A20-B19] linkages were found. The corresponding segments from the digestion products of [ΔA19Tyr]-HPI were also found as shown in Fig. 3. These results indicate that the shifted A19-B19 disulfide bond in [ΔA19Tyr]-HPI exists exactly as expected.

Comparison of the In Vitro Refolding of Native and Mutant HPIs—HPI and mutant HPIs were fully reduced by DTT and then dialyzed against the refolding buffer (pH 10.8) for renaturation. The *in vitro* refolding products were analyzed by native PAGE as shown in Fig. 2B. The relative percentage of the band representing the correctly refolded product was quantified by densitometry, and the refolding yields are summarized in Fig. 2C. There are significant differences between the refolding yields of the two mutant HPIs and that of native HPI. Deletion of the A20-B19 disulfide bond resulted in a decrease in the refolding yield to about 45%, while deletion of A19Tyr in [ΔA19Tyr]-HPI dramatically decreased the refolding yield to about 7%. The same result can be seen for the non-reductive SDS-PAGE assay of refolded products (Fig. 2D). Apart from the monomeric product, the refolding of HPI and its two mutants also gave dimers and other polymers to different degrees. Although reduced [A20, B19Ala]-HPI has only four thiol groups, the refolding products included much more polymeric material with much less correctly folded monomer. Meanwhile, with six thiol groups, the refolding of [ΔA19Tyr]-HPI resulted in the most products in polymeric form.

In Vitro Oxidation of Reduced Proteins—Figure 4 shows the time courses of the oxidation of reduced HPI and mutant HPIs. During the first half-hour of refolding, the thiol groups of reduced [A20, B19Ala]-HPI and [ΔA19Tyr]-HPI were both oxidized at a high speed similar to that of HPI. Because neither of the two mutants have mutations to the A6-A11 disulfide bond, this result

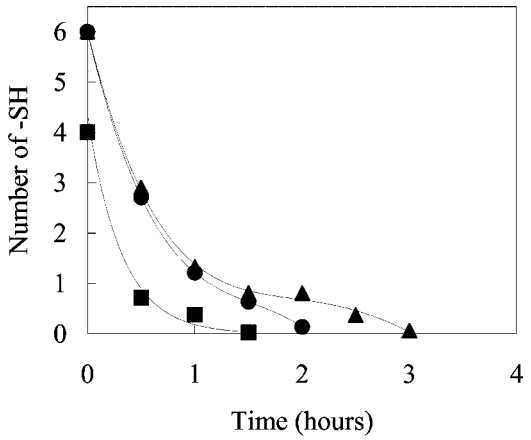

Fig. 4. **Time course of the oxidation of reduced HPI and its analogues.** The values represent the means of data in triplicate. Circles, squares, triangles represent HPI, [A20, B19Ala]-HPI, and [ΔA19Tyr]-HPI, respectively.

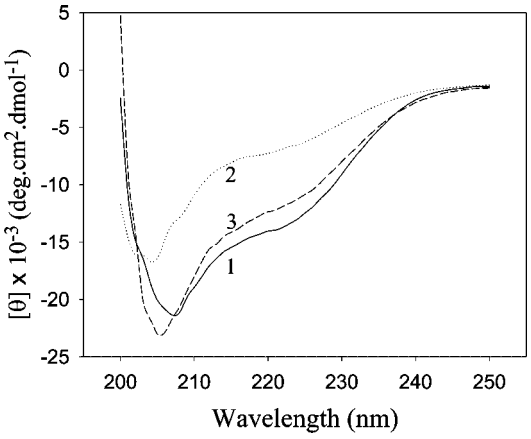

Fig. 5. **CD spectra of HPI and its analogues.** The spectra are the averages of four scans from 200 to 250 nm. Traces 1, 2, and 3 represent HPI, [A20, B19Ala]-HPI, and [ΔA19Tyr]-HPI, respectively.

agrees with previous findings that the intra-A chain disulfide bond forms first at high speed (*8*). One hour after the beginning of refolding, the oxidation of [ΔA19Tyr]-HPI became slower than that of HPI, while the oxidation of [A20, B19Ala]-HPI remained similar to that of HPI. Since most of the *in vitro* refolding products of both mutants were in polymeric form, the oxidation of the thiol groups in the late stage can be taken as mainly involving intermolecular reactions.

CD Spectra of Native and Mutant HPIs—CD spectra are often used to monitor changes in the secondary structure of proteins. In order to see the effect of mutation of

Table 1. **Secondary structure content of native and mutant HPIs.**

Structure content (%)	α-helix	β-sheet	Random coil
HPI	39.1	7.7	53.3
[A20-B19Ala]-HPI	7.5	33.6	58.9
[ΔA19Tyr]-HPI	30.9	7.3	61.8

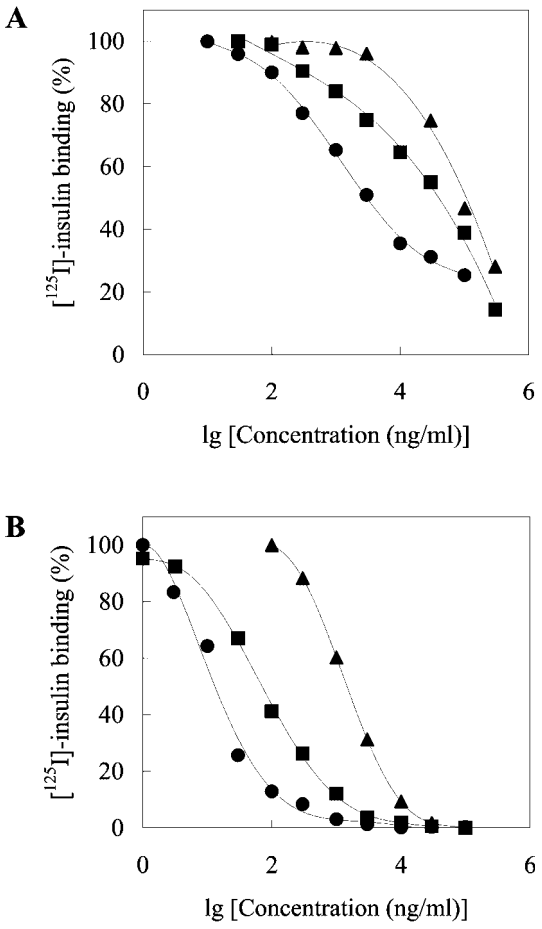

Fig. 6. **Receptor and antibody binding assays of HPI and its analogues.** The values represent means of data in triplicate. (A) receptor binding assay, (B) antibody binding assay. In each panel, circles, squares, and triangles represent HPI, [A20, B19Ala]-HPI, and [ΔA19Tyr]-HPI, respectively.

the A20-B19 disulfide bond on the structure of proinsulin, CD spectra were recorded (Fig. 5) and the relative secondary structure contents were calculated and listed in Table 1. The α-helix content of the deletion mutant [A20, B19Ala]-HPI decreased to 7.5%, much lower than the 39.1% α-helix content of native HPI. This indicates that [A20, B19Ala]-HPI may assume a conformation that is much looser than that of HPI. However, the secondary structure content of [ΔA19Tyr]-HPI is slightly lower than that of HPI, which suggests that it retains a reasonably compact conformation.

In Vitro Receptor and Antibody Binding Activities—Results of receptor and antibody binding assays are shown in Fig. 6 and the relative activities of the HPI mutants compared with native HPI are summarized in

Table 2. **Receptor and antibody binding activities of mutant HPIs as compared with HPI.**

	Receptor binding activity (%)	Antibody binding activity (%)
[A20-B19Ala]-HPI	7	24
[ΔA19Tyr]-HPI	3 (3.6)	0.8 (2)

Data in parentheses are activities compared with Lys-HPI (*21*).

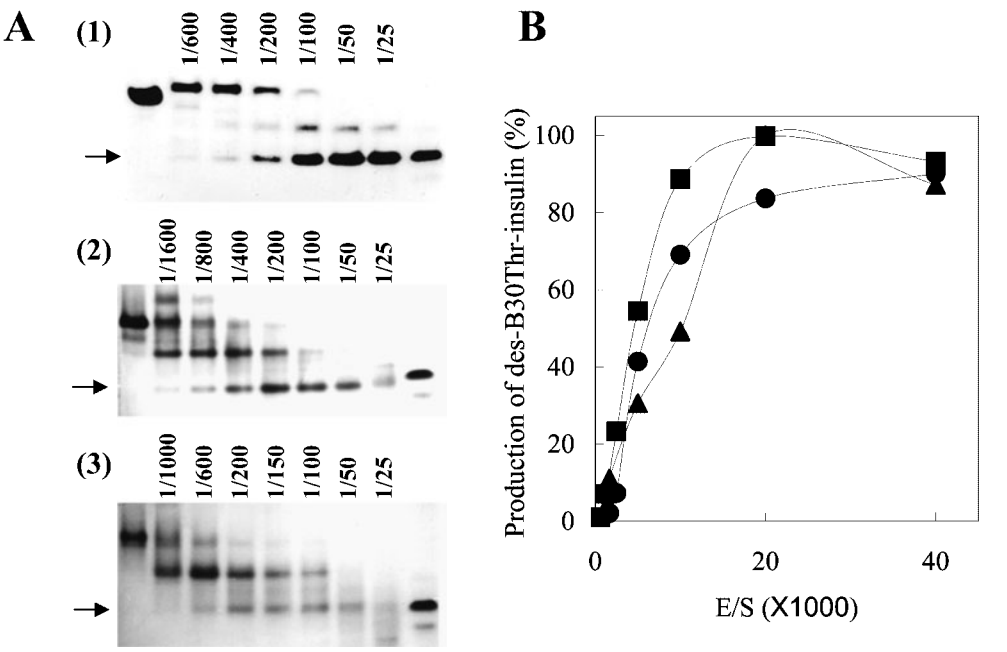

Fig. 7. **Electrophoretic analysis of tryptic digestion products of HPI and its analogues.** (A) 15% native PAGE analysis of the tryptic products of HPI and its analogues at different E/S ratios. 1, 2, and 3 represent HPI, [A20, B19Ala]-HPI, and [ΔA19Tyr]-HPI, respectively. In each panel, the far-left lane is HPI or the corresponding mutant analogue, the far-right lane is porcine insulin used as a control. Enzyme/substrate (w/w) ratios are marked at the top of each lane. The lanes for des-B30Thr-insulin and its analogues are indicated by arrows. (B) a plot indicating the formation of des-B30Thr-insulin analogues for each mutant HPI analogue at different E/S ratios. Curves circles, squares, triangles represent HPI, [A20, B19Ala]-HPI, and [ΔA19Tyr]-HPI, respectively.

Table 2. [A20, B19Ala]-HPI shows some binding activity to insulin receptor and 24% binding activity to insulin antibody. As for [ΔA19Tyr]-HPI, after excluding the influence of the additional N-terminal lysine on the biological activity of HPI (*21*), it was shown that both of the receptor and antibody binding activities decrease greatly.

Sensitivity of Mutant HPIs to Tryptic Digestion—Purified HPI and mutant HPIs were digested with trypsin, and analyzed by native PAGE (Fig. 7A). The tryptic mapping pattern of the mutant HPIs were similar to that of HPI as all proteins share the same tryptic cleaving sites. Des-B30Thr-insulin as well as some intermediates could be observed during tryptic digestion. First, in contrast with the much lower mobility rate of [ΔA19Tyr]-HPI than that of HPI, the mobility rate of des-B30Thr-[ΔA19Tyr]-insulin is similar to that of porcine insulin on native PAGE [Fig. 7A (*3*)]. Because trypsin digestion removes the additional N-terminal lysine of [ΔA19Tyr]-HPI, this agrees with the CD data that indicate [ΔA19Tyr]-HPI to have a relatively compact conformation. The production of des-B30Thr-insulin analogues at different enzyme/substrate ratios was quantified from the gels and the results are plotted in Fig. 7B. Compared with HPI, the [A20, B19Ala]-HPI and [ΔA19Tyr]-HPI analogues were both more sensitive to trypsin digestion. [A20, B19Ala]-HPI digested more easily than HPI at any enzyme/substrate ratio. In the case of [ΔA19Tyr]-HPI, the amount of released des-B30Thr-insulin was similar to or less than that from the HPI digestion at lower enzyme/substrate ratios, while at higher enzyme/substrate ratios, [ΔA19Tyr]-HPI was obviously more sensitive to trypsin digestion than HPI.

DISSCUSION

Disulfide bonds in proteins usually serve as a major element for structural stabilization. In the case of insulin, the three disulfide bonds are absolutely conserved throughout its molecular evolution. It was found that deletion of the A6–A11 intra-A chain disulfide bond results in an unfolding of the N-terminal α-helix of the insulin A chain and a great decrease in biological activity (*5–7*). Deletion of the A7-B7 inter-chain disulfide bond results in the unfolding of all the A-chain N-terminal α-helix and part of the C-terminal α-helix, and, therefore, leads to more serious effects on structure and biological activity than deletion of the A6-A11 disulfide bond (*9–11*). In this study, the significant decrease in the α-helix content of [A20, B19Ala]-HPI suggests that deletion of the A20–B19 disulfide bond leads to a much looser conformation of the proinsulin molecule. This also agrees with the result that [A20, B19Ala]-HPI migrates more slowly than HPI in native-PAGE gel and is more sensitive to tryptic digestion than HPI. These findings indicate that the A20-B19 inter-chain disulfide bond plays an important role in stabilizing the structure of insulin/proinsulin. Comparison of the CD spectra of HPI analogues with deletion mutations in either the A6–A11 or A7–B7 disulfide bond, as reported previously (*11*, *12*), shows that the decrease in the α-helix content of [A20, B19Ala]-HPI is the most serious among the one-disulfide-bond-deleted HPI mutants. This suggests that the A20–B19 disulfide bond is the most important element for structure stabilization among the three disulfide bonds of insulin. This also agrees with the conclusions of studies on the PIP mutant with only the A20–B19 disulfide bond (*15*). Moreover, our results show that the mutant with a shifted A20–B19 disulfide bond [ΔA19Tyr]-HPI still retains a compact conformation, which also suggests an important role of such an inter-chain disulfide bond in structure stabilization.

A specific molecular conformation of a protein is the basis for its biological functions. It has been found that deletion of either the A6–A11 or A7–B7 disulfide bond greatly decreases the binding activity of proinsulin to insulin receptor (*11*, *12*). In this study, the receptor bind-

ing activity of [A20, B19Ala]-HPI decreased, but not as much as mutants with deletions in the A6–A11 or A7–B7 disulfide bond. This agrees with the previous conclusion that the A-chain N-terminal α-helix is important for the interaction with the insulin receptor (*22*). Deletion of the A20-B19 disulfide bond loosens the structure of the whole molecule, but causes less effect on the local structure of the A-chain N-terminal α-helix than deletion of the A6–A11 or A7–B7 disulfide bond. Changes in immunological activity may reflect more global conformational changes in a protein molecule. Although our results showed that [ΔA19Tyr]-HPI has a more compact conformation, its biological activity, especially its antibody binding activity, is very low. This indicates that the conformation of [ΔA19Tyr]-HPI is quite different with that of native HPI. A similar result was obtained in our previous study on [ΔA19Tyr]-insulin and concluded to be an effect of A19Tyr deletion (*16*). Since global conformational changes have been reported in many recent studies on insulin isomers and other HPI mutants with shifted disulfide bonds (*12*, *23*, *24*), we deduce that the global conformational changes of [ΔA19Tyr]-HPI are mainly due to the shift mutation in the A20–B19 disulfide bond.

In a recent study on the captured refolding intermediates of human HPI, a three-disulfide-bond intermediate with a native A20–B19 disulfide bond was proved to be essential in the folding pathway from other captured intermediates to native HPI (*14*). Our results shown here prove the important role of the A20–B19 disulfide bond in the refolding of HPI directly. The refolding yields of HPI decreased significantly when the A20–B19 disulfide bond was mutated. However, in previous studies conducted under the same conditions, all the A6–A11 or A7–B7 disulfide bond mutants showed little effects on the refolding yields of HPI (*12*). In contrast with HPI mutants with a shifted A6–A11 or A7–B7 disulfide bond (*12*), the refolding yields of [ΔA19Tyr]-HPI are extremely low, indicating that the formation of the shifted disulfide bond A19–B19 is quite difficult for HPI, which may be due to the existence of a high energy barrier. This also suggests that the correct formation of the A20–B19 disulfide bond is important in the folding of proinsulin.

Although a folding pathway of HPI was recently proposed by study of several captured folding intermediates, the details remain unknown due to the limited types of captured intermediates. On the other hand, so far, deletion or shifted mutations have been introduced to each of the three disulfide bonds of insulin or proinsulin (*8–12*). *In vitro* refolding studies on these disulfide bond mutants have also provided much information about the refolding pathway of proinsulin. By combining this refolding information from mutants with results of other studies on proinsulin refolding, a possible folding pathway of HPI can be proposed: In the initial stage of the folding process, the intra-A chain disulfide bond A6–A11 forms first very quickly, stabilizing a partially folded A-chain secondary structure (*8*, *13*); the C-peptide may serves as an intra-molecular chaperon (*20*) to assist A chain pairing with the folded B-chain, which serves as a folding template (*10*, *25*); nonnative disulfide bonds then form and reshuffle until the formation of the native A20–B19 interchain disulfide bond (*14*), and the primary molecular conformation is assumed; finally, the flexibility in the region of the [A6-A11, A7-B7] disulfide bond facilitates the formation of the native A6–A11 and A7–B7 disulfide bonds (*12*).

This work was supported by a grant from National Natural Science Foundation of China (30170204) to J.G. Tang.

REFERENCES

1. Rosenfeld, R.D., Miller, J.A., Narhi, L.O., Hawkins, N., Katta, V., Lauren, S., Weiss, M.A., and Arakawa, T. (1997) Putative folding pathway of insulin-like growth factor-I. *Arch. Biochem. Biophys.* **342**, 298–305
2. Narhi, L.O., Hua, Q.X., Arakawa, T., Fox, G.M., Tsai, L., Rosenfeld, R., Holst, P., Miller, J.A., and Weiss, M.A. (1993) Role of native disulphide bonds in the structure and activity of insulin-like growth factor 1: genetic models of protein-folding intermediates. *Biochemistry* **32**, 5214–5221
3. Hober, S., Forsberg, G., Palm, G., Hartmanis, M., and Nilsson, B. (1992) Disulphide exchange folding of insulin-like growth factor I. *Biochemistry* **31**, 1749–1756
4. Milner, S.J., Carver, J.A., Ballard, F.J., and Francis, G.L. (1999) Probing the disulfide folding pathway of insulin-like growth factor-I. *Biotechnol. Bioeng.* **62**, 693–703
5. Dai, Y. and Tang, J.G. (1994) Intra-A chain disulfide bond (A6-11) of insulin is essential for displaying its activity. *Biochem. Mol. Biol. Int.* **33**, 1049–1053
6. Dai, Y. and Tang, J.G. (1996) Characteristic, activity and conformational studies of [A6-Ser, A11-Ser]-insulin. *Biochim. Biophys. Acta* **1296**, 63–68
7. Hua, Q.X., Hu, S.Q., Frank, B.H., Jia, W., Chu, Y.C., Wang, S.H., Burke, G.T., Katsoyannis, P.G., and Weiss, M.A. (1996) Mapping the functional surface of insulin by design: structure and function of a novel A-chain analogue. *J. Mol. Biol.* **264**, 390–403
8. Yuan, Y., Wang, Z.H., and Tang, J.G. (1999) Intra-A chain disulphide bond forms first during insulin precursor folding. *Biochem. J.* **343**, 139–144
9. Guo, Z.Y. and Feng, Y.M. (2001) Effects of cysteine to serine substitutions in the two inter-chain disulphide bonds of insulin. *Biol. Chem.* **382**, 443–448
10. Hua, Q.X., Nakagawa, S.H., Jia, W., Hu, S.Q., Chu, Y.C., Katsoyannis, P.G., and Weiss, M.A. (2001) Hierarchical protein folding: asymmetric unfolding of an insulin analogue lacking the A7-B7 interchain disulfide bridge. *Biochemistry* **40**:12299–12311
11. Liu, Y. and Tang, J.G. (2003) Influence of A7-B7 disulfide bond deletion on the refolding and structure of proinsulin. *Acta Bioch. Bioph. Sin.* **35**, 122–126
12. Liu, Y., Wang, Z.H., and Tang, J.G. (2003) Flexibility exists in the region of [A6-A11, A7-B7] disulfide bonds during insulin precursor folding. *J. Biochem.* (in press)
13. Qiao, Z.S., Guo, Z.Y., and Feng, Y.M. (2001) Putative disulphide-forming pathway of porcine insulin precursor during its refolding *in vitro*. *Biochemistry* **40**, 2662–2668
14. Qiao, Z.S., Min, C.Y., Hua, Q.X., Weiss, M.A., and Feng, Y.M. (2003) *In vitro* refolding of human proinsulin: kinetic intermediates, putative disulfide-forming pathway, folding initiation site and potential role of C-peptide in folding process. *J. Biol. Chem.* **278**, 17800–17809
15. Yan, H., Guo, Z.Y., Gong, X.W., Xi, D., and Feng, Y.M. (2003) A peptide model of insulin folding intermediate with one disulfide. *Protein Sci.* **12**, 768–775
16. Du, X. and Tang, J.G. (1998) Effects of deleting A19 tyrosine from insulin. *Biochem. Mol. Biol. Int.* **44**, 507–513
17. Tang, J.G. and Hu, M.H. (1993) Production of human proinsulin in *E. coli* in a non-fusion form. *Biotechnol. Lett.* **15**, 661–666
18. Ellman, G.L. (1959) Tissue sulfhydryl groups. *Arch. Biochem. Biophys.* **82**, 70–77
19. Chen, Y.H., Yang, J.T., and Martinez, H.M. (1972) Determination of the secondary structures of proteins by circular dichr-

oism and optical rotatory dispersion. *Biochemistry* **11**, 4120–4131
20. Chen, L.M., Yang, X.W., and Tang, J.G. (2002) Acidic residues on the N-terminus of proinsulin C-peptide are important for the folding of insulin precursor. *J. Biochem.* **131**, 855–859
21. Tang, J.G., Zhang, H.T., Sun, H.Y., D., Y., and H., M.H. (1994) Modification of N-terminus of insulin B chain and its possible biological function. *Chinese Biochem. J.* **10**, 665–669
22. Olsen, H.B., Ludvigsen, S., and Kaarsholm, N.C. (1998) The relationship between insulin bioactivity and structure in the NH_2-terminal A-chain helix. *J. Mol. Biol.* **284**, 477–488
23. Hua, Q.X., Gozani, S.N., Chance, R.E., Hoffmann, J.A., Frank, B.H., and Weiss, M.A. (1995) Structure of a protein in a kinetic trap. *Nat. Struct. Biol.* **2**, 129–138
24. Hua, Q.X., Jia, W., Frank, B.H., Phillips, N.F., and Weiss, M.A. (2002) A protein caught in a kinetic trap: structures and stabilities of insulin disulfide isomers. *Biochemistry* **41**, 14700–14715
25. Guo, Z.Y., Shen, L., and Feng, Y.M. (2002) The different folding behavior of insulin and insulin-like growth factor 1 is mainly controlled by their B-chain/domain. *Biochemistry* **41**, 1556–1567